



Machine Learning-Based PV Reserve Determination Strategy for Frequency Control on the WECC System

Preprint

Haoyu Yuan,¹ Jin Tan,¹ Yingchen Zhang,¹
Samanvitha Murthy,¹ Shutang You,² Hongyu Li,² Yu Su,²
and Yilu Liu³

¹ *National Renewable Energy Laboratory*

² *University of Tennessee, Knoxville*

³ *Oak Ridge National Laboratory*

*Presented at the 2020 IEEE Conference on Innovative Smart Grid Technologies (IEEE ISGT)
Washington, D.C.
February 17–20, 2020*

**NREL is a national laboratory of the U.S. Department of Energy
Office of Energy Efficiency & Renewable Energy
Operated by the Alliance for Sustainable Energy, LLC**

This report is available at no cost from the National Renewable Energy Laboratory (NREL) at www.nrel.gov/publications.

Contract No. DE-AC36-08GO28308

Conference Paper
NREL/CP-5D00-74829
July 2020



Machine Learning-Based PV Reserve Determination Strategy for Frequency Control on the WECC System

Preprint

Haoyu Yuan,¹ Jin Tan,¹ Yingchen Zhang,¹
Samanvitha Murthy,¹ Shutang You,² Hongyu Li,² Yu Su,²
and Yilu Liu³

¹ *National Renewable Energy Laboratory*

² *University of Tennessee, Knoxville*

³ *Oak Ridge National Laboratory*

Suggested Citation

Yuan, Haoyu, Jin Tan, Yingchen Zhang, Samanvitha Murthy, Shutang You, Hongyu Li, Yu Su, and Yilu Liu. 2019. *Machine Learning-Based PV Reserve Determination Strategy for Frequency Control on the WECC System: Preprint*. Golden, CO: National Renewable Energy Laboratory. NREL/CP-5D00-74829. <https://www.nrel.gov/docs/fy20osti/74829.pdf>.

© 2020 IEEE. Personal use of this material is permitted. Permission from IEEE must be obtained for all other uses, in any current or future media, including reprinting/republishing this material for advertising or promotional purposes, creating new collective works, for resale or redistribution to servers or lists, or reuse of any copyrighted component of this work in other works.

**NREL is a national laboratory of the U.S. Department of Energy
Office of Energy Efficiency & Renewable Energy
Operated by the Alliance for Sustainable Energy, LLC**

This report is available at no cost from the National Renewable Energy Laboratory (NREL) at www.nrel.gov/publications.

Contract No. DE-AC36-08GO28308

Conference Paper
NREL/CP-5D00-74829
July 2020

National Renewable Energy Laboratory
15013 Denver West Parkway
Golden, CO 80401
303-275-3000 • www.nrel.gov

NOTICE

This work was authored in part by the National Renewable Energy Laboratory, operated by Alliance for Sustainable Energy, LLC, for the U.S. Department of Energy (DOE) under Contract No. DE-AC36-08GO28308. Funding provided by U.S. Department of Energy Solar Energy Technologies Office Award Number 34231. The views expressed herein do not necessarily represent the views of the DOE or the U.S. Government. The U.S. Government retains and the publisher, by accepting the article for publication, acknowledges that the U.S. Government retains a nonexclusive, paid-up, irrevocable, worldwide license to publish or reproduce the published form of this work, or allow others to do so, for U.S. Government purposes.

This report is available at no cost from the National Renewable Energy Laboratory (NREL) at www.nrel.gov/publications.

U.S. Department of Energy (DOE) reports produced after 1991 and a growing number of pre-1991 documents are available free via www.osti.gov.

Cover Photos by Dennis Schroeder: (clockwise, left to right) NREL 51934, NREL 45897, NREL 42160, NREL 45891, NREL 48097, NREL 46526.

NREL prints on paper that contains recycled content.

Machine Learning-Based PV Reserve Determination Strategy for Frequency Control on the WECC System

Haoyu Yuan, Jin Tan, Yingchen Zhang, and
Samanvitha Murthy¹
National Renewable Energy Laboratory
Golden, CO, USA
{haoyu.yuan, jin.tan,
yingchen.zhang}@nrel.gov and
samanvim@andrew.cmu.edu

Shutang You, Hongyu Li, and Yu Su
² Department of Electrical Engineer and
Computer Science
University of Tennessee, Knoxville
Knoxville, TN, USA
{syou3, hli90, ysu10}@utk.edu

Yilu Liu^{2,3}
³ Oak Ridge National Laboratory
Oak Ridge, TN, USA
liu@utk.edu

Abstract—Frequency control from photovoltaic (PV) power plants has great potential to address the frequency response challenge of the power system with high penetrations of renewable generation. Using model-based approaches to determine the optimal PV headroom reserve, however, requires significant online computation and is intractable for an interconnection level system. This paper proposes a machine learning based strategy, that is suitable for real-time operation, to determine the optimal PV reserve for frequency control. The proposed machine learning algorithm is trained and tested on 1,987 offline simulations of a 60% renewable penetration Western Electricity Coordinating Council (WECC) system. Furthermore, the proposed reserve determination strategy is applied on a realistic 1-day operation profile of the WECC system and demonstrates a savings of more than 40% PV headroom compared to a conservative approach. It is evident that the proposed strategy can efficiently and effectively determine the optimal PV frequency control reserve for realistic interconnection systems.

Keywords—frequency control, machine learning, neural network, photovoltaic (PV), renewable energy, reserve, WECC.

I. INTRODUCTION

Driven by aggressive renewable portfolio standards [1] as well as competitive costs of renewable generation technologies, renewable energy installation has increased in recent years at a record pace. Among various technologies, photovoltaic (PV) power has been a major contributor because of its increasing competitiveness against other technologies. Notably, the U.S. Department of Energy (DOE) SunShot vision study estimated that solar generation could provide up to 27% energy by 2050 [2]. Under this scenario, the instantaneous PV penetration could reach 70% or more assuming a capacity factor of 0.2 [3].

Meanwhile, high penetration levels of inverter-based resource (IBR), such as PV, along with the retirement of synchronous generators, has brought new challenges to the bulk electric system. In particular, the frequency response will be negatively impacted as a result of reduced inertia and governor response from synchronous generators. A recent study observed deteriorated frequency responses of the three main U.S. interconnections under ultra-high penetrations of IBR [3].

One practical solution to address the frequency response challenge is to enable frequency control for inverter-based renewable energy resources. A comprehensive review of the technical capabilities of variable speed wind turbines and solar PV generators was given in [4]. Moreover, frequency control along with other controls was demonstrated on a 300 MW

utility-scale PV power plant in California in [5], showing that PV power plants are technically capable of providing frequency response when necessary headroom is reserved.

However, how much headroom should PV plants reserve during real-time operation in order to meet system performance requirements has rarely been explored. Throughout the course of a day, unit commitment and dispatch are constantly changing in response to load and renewable resource fluctuation. As a result, the online inertia and enabled governor capacity from synchronous generators can vary significantly, which makes it challenging for system operators to determine the PV headroom reserve requirement in real-time operation.

Using model-based simulations of numerous scenarios to determine the reserve requirement in real time is computationally intense and become intractable for interconnection level systems with tens of thousands of buses. Lacking the capability of real-time assessment, system operators will need to procure a conservative amount of headroom reserve, which will incur opportunity costs of the overly procured PV headroom reserve not providing energy.

To address the challenge of determining real-time PV reserve requirement, this paper proposes a machine learning-based strategy that is applicable to interconnection level power systems. First, a large offline training database is created through dynamic simulations on the WECC 2022 60% IBR case developed under the DOE SunShot National Laboratory Multiyear Partnership (SuNLaMP) program [6]. Then an algorithm based on Artificial Neural Network (ANN) is trained and tested on this data set. Finally, to validate the effectiveness of the proposed strategy, it is applied to a realistic 1-day operation profile of the WECC system that is never seen by the machine learning model during the offline training. The results show that, on one hand, the PV headroom determination strategy generalizes well to the unseen one-day profile by meeting the required system frequency response; on the other hand, it achieves a savings of more than 40% PV reserve compared with a conservative strategy.

The remainder of this paper is organized as follows. Section II introduces the proposed machine learning-based PV headroom determination strategy. Section III describes the offline training of the machine learning-based algorithm on the WECC system with high IBR penetration. Section IV demonstrates the online application of the proposed strategy during a realistic one-day operation. Section V concludes this paper.

¹ Samanvitha Murthy is also with Carnegie Mellon University.

II. MACHINE LEARNING-BASED PV RESERVE DETERMINATION STRATEGY FOR FREQUENCY CONTROL

A. PV Frequency Control

The technical feasibility of using PV to provide frequency control has been proven [3]–[5]. Broadly, frequency control injects power to help arrest the decline of system frequency during an under-frequency event such as generation trip. The inertia control and primary frequency control of the PV power plant used in this paper are shown in Fig. 1. The following control parameters are used: $[K_i, T_{lpwi}, T_{wowi}, P_{mxwi}, P_{mnwi}, K_g, T_{lpwg}, T_{wogw1}, T_{wogw2}, db_i, db_g] = [38, 0.5, 1.5, 0.1, 0, 20, 0.1, 0.3, 0.5, 0, 0.0006]$.

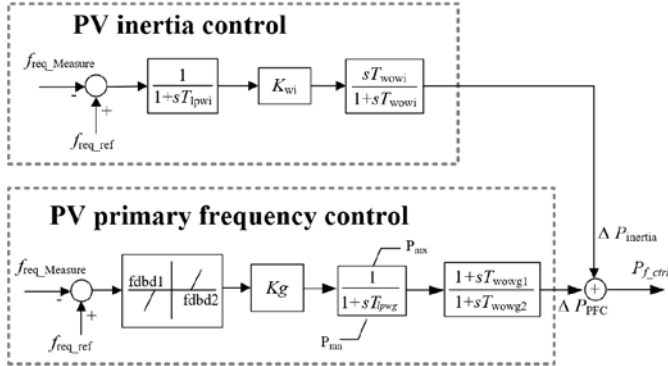


Fig. 1. Block of PV frequency control

To provide upward frequency control, PV plants are required to pre-curtail and maintain headroom. For a better illustration, Fig. 2 shows the system frequency nadirs of a small test system under the same generation trip but with different amounts of PV headroom reserve. As the PV headroom increases, the frequency nadir improves at the beginning but stays constant after a certain point at which the control cannot use 100% of the reserved headroom. It is beneficial to system frequency response to reserve more PV headroom until a certain point; however, because a PV plant does not have a fuel cost to generate electricity, reserving an excessive amount of PV headroom is uneconomic. Therefore, it is necessary to develop a method that can determine the appropriate amount of PV headroom.

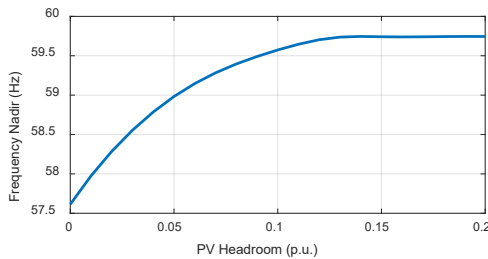


Fig. 2. Frequency nadir under the generation trip with different PV headroom.

B. Machine Learning-Based Strategy

One key performance metric in frequency stability analysis is the frequency nadir, f_{nadir} , which is defined as the minimum post-contingency frequency. In practice, the frequency nadir under the worst credible contingency should be maintained above the under-frequency load-shedding (UFLS) settings so that the worst contingency will not activate any load shedding. The proposed PV headroom dispatch strategy has the objective

to choose the minimum PV headroom while meet the predefined frequency nadir.

From the physical model of the power system, the total system inertia of online synchronous generators and the enabled governor capacity are the two main factors that impact the frequency nadir. Therefore, the machine learning algorithm is designed to use the input of the targeted frequency nadir, f_{target} , online system inertia, H_{system} , and online governor capacity, G_{gov} , to determine the PV headroom, HR_{PV} .

After the objective and input to the machine learning-based strategy is clear, the strategy is further divided into offline training and online application modules, which is illustrated in Fig. 3.

The offline training module consists of the creation of a frequency stability database, i.e. the training data, and the machine-learning model training process. Dynamic simulations of different combinations of $(H_{system}, G_{gov}, HR_{PV})$ will be performed to generate the training data. Then the machine learning algorithm will be trained accordingly.

In the online application module, the machine learning algorithm will be deployed in the control room. Real-time streaming data of totally system inertia and enabled governor capacity will be input to the machine learning algorithm. Also, the system operator will set a desired frequency nadir. The machine learning algorithm will determine an optimal amount of PV headroom, and then the system operator will distribute the headroom to the PV power plant controllers.

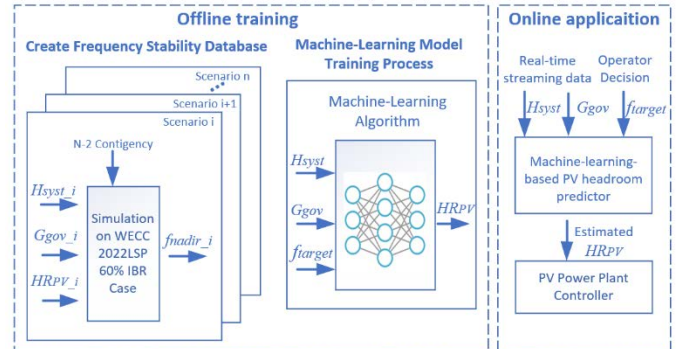


Fig. 3. Flow chart of the proposed strategy.

III. OFFLINE TRAINING ON THE WECC SYSTEM

One challenge of directly training a regression model between $(f_{target}, H_{system}, G_{gov})$ and HR_{PV} is that, in the dynamic simulation, HR_{PV} is naturally an independent variable, i.e. input to the simulation, and the frequency nadir, f_{nadir} , is a dependent variable, i.e. a result of the simulation. As shown in Fig. 3, the training data set is structured to have three features $(H_{system}, G_{gov}, HR_{PV})$ and one label f_{nadir} . As a result, this creates a discrepancy between the training data structure and the regression model. To cope with this challenge, a two-step approach is proposed:

Step 1: intuitively, a Neural Network (NN) regression model between $(H_{system}, G_{gov}, HR_{PV})$ to f_{nadir} is trained.

Step 2: a binary search algorithm is developed that searches the minimum HR_{PV} through the NN regression model to meet the f_{target} under the input of (H_{system}, G_{gov}) .

A. Create Frequency Stability Database

For a machine learning algorithm to achieve good performance in online application, the training set needs to cover operation conditions in the field. In this application, this means realistic ranges of $(H_{\text{sys}}, G_{\text{gov}}, HR_{\text{PV}})$ needs to be simulated.

The U.S. WECC system high PV model used in this project was developed by the SuNLaMP project 30844 and is a detailed planning model based on the 2022 light spring case. This case has 60% penetration of IBRs, including 45% PV and 15% wind. Because the current WECC system does not have such a high penetration of IBRs, the ranges of system inertia and enabled governor capacity of today's system will differ from the ranges of the system in 2022; however, a reasonable projection of the future can be made based on current condition.

A typical 1-day inertia trend of the current WECC system (from the North American Electric Reliability Corporation) is depicted by the blue curve in Fig. 4. As the PV penetration increases, more synchronous generators will be decommitted during the peak hours of PV which will lead to decreased H_{sys} and G_{gov} . To reflect this impact, for every 1% PV penetration increase, 1% of inertia decrease and 1% of enabled governor capacity decrease are assumed. To project the future PV profile, a 24-hour PV profile of the California region is retrieved from the California Independent System Operator (CAISO) OASIS website [7] and is scaled to fit the PV generation of the high penetration case. This is depicted by the yellow curve on the right axis. As a result, the projected system inertia is calculated and depicted as the red curve.

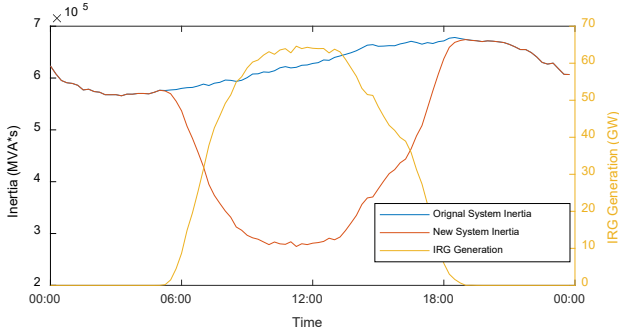


Fig. 5. One-day profile of the WECC system.

Based on the projected inertia profile, the range of inertia is chosen to be $[260,000, 740,000]$ (MVA·s) to cover the entire range of the projection. A step of 40,000 MVA·s is chosen which leads to 13 steps.

At the same time, the range of the enabled governor capacity is scaled proportional to the inertia and a range of $[19,000, 67,000]$ (MVA) is determined. A step of 3,000 MVA is chosen which leads to 17 steps.

To determine the range of PV headroom, simulations on the system condition with lowest inertia and enabled governor capacity are performed by varying the PV headroom from 0% to 4% with a 0.5% step. The average frequency responses of 22 buses across the system are recorded and plot in Fig. 5. As shown, this range covers the frequency nadir from 59.4 Hz to 59.9 Hz which creates a 0.5-Hz frequency range from which operators have the flexibility to choose the frequency target.

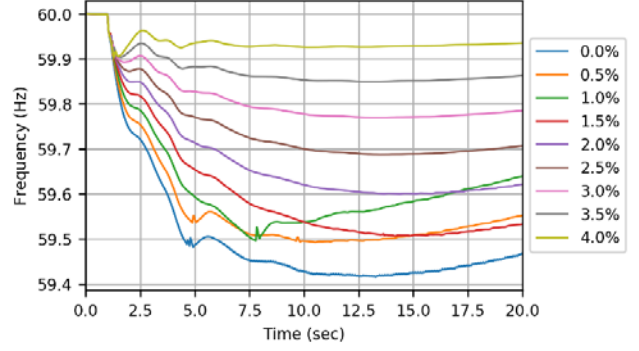


Fig. 4. Frequency responses under different headroom reserve levels

Therefore, it is reasonable to simulate $[0.0\%, 4.0\%]$. A 0.5% step is used which lead to 9 steps.

There are 13 inertia levels, 17 governor capacity levels, and 9 headroom levels, which creates 1,989 combinations to simulate. For each simulation, the largest N-2 contingency—which is the loss of two generating units in the Palo Verde nuclear plant (2600 MW)—is simulated for 20 seconds. The average frequency of the selected 22 buses is calculated and frequency nadir is found as the lowest average frequency during the 20 seconds simulation.

Simulations are performed through the GE Positive Sequence Load Flow (PSLF) software on a virtual machine equipped with Intel Xeon Gold 6148 CPU @ 2.40 GHz and a RAM of 6 GB. It took the virtual machine 14 days' time to finish all 1,989 simulations.

Note that only the inertia range of the 1-day profile is used to determine the range of the training data. The actual operating conditions of $(H_{\text{sys}}, G_{\text{gov}}, HR_{\text{PV}})$ throughout the day are never seen by the machine learning algorithms.

B. Training Artificial Neural Network Regression Model

An ANN model is chosen as the regression model. Open-source machine learning packages in Python language are used: the scikit-learn [8] package is used for the scaler, grid search, and cross validation process; the TensorFlow [9] package is used as the backend of the neural network algorithms; and Keras [10] package is used as the high-level application programming interface.

Histograms of the four attributes of the 1,989 simulations are shown in Fig. 6. The three inputs, i.e. H_{sys} , G_{gov} , and HR_{PV} , are distributed evenly across the levels defined in subsection A. Except two outliers around 59.0 Hz, frequency nadirs, are distributed between $[59.4, 59.95]$, which justifies the PV headroom range chosen in Subsection A. Further examination of the two outliers shows that the frequency of one bus is significantly distorted and thus unrealistically low compared with the frequencies of the other 21 buses. The two extreme low frequencies could be caused by the algorithm that calculates the bus frequency in PSLF and are removed from training or testing. Among the remaining 1,987 instances, 20% is set aside as the test set and the other 80% is used as the training set.

In the ANN model, only one hidden layer is used because of the small number of inputs and output. The rectified linear unit

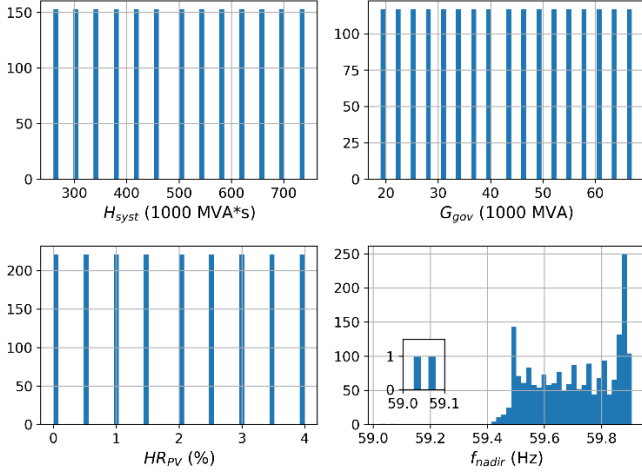


Fig. 6. Histograms of features.

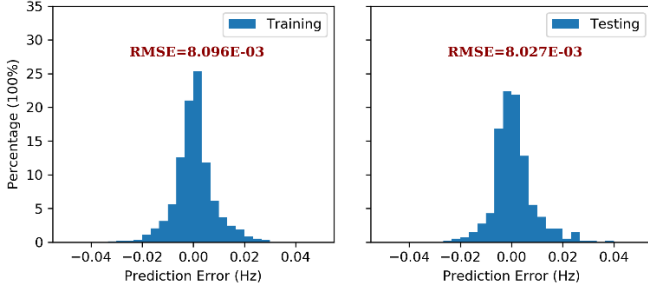


Fig. 7. Prediction errors of training and testing cases.

(ReLU) activation function is used in the hidden layer and linear activation function is used in the output layer. Mean square error is used as the loss function. To avoid overfitting, l_2 regularization is added in the model, and five-fold cross-validation is implemented during training.

To fine-tune the model, grid search on the following hyperparameters are performed to find the optimal settings: number of neurons in the hidden layer, n_h : [25, 50, 100]; regularization parameter, λ : [0.01, 0.005, 0.001]; batch size, b : [10, 20, 30]; and number of epochs, n_e : [50, 100, 150]. The best training result is achieved with $[n_h, \lambda, b, n_e] = [50, 0.001, 10, 150]$. The prediction errors of the fine-tuned NN model on both the training and testing data are illustrated using the histograms shown in Fig. 7 and are bounded by ± 0.04 Hz. The root mean square errors (RMSE) of the predictions on the training and testing set are $8.096E-03$ Hz and $8.027E-03$ Hz which are both less than 0.01 Hz. It is demonstrated that the ANN model performs consistently well on both training and testing data.

C. Binary Search Algorithm

On top of the fine-tuned ANN model, a binary search algorithm is developed to search the optimal PV headroom to meet the frequency nadir target, f_{target} . The search algorithm is illustrated through the flowchart in Fig. 8.

The algorithm takes the input of $(f_{target}, H_{syst}, G_{gov})$ and two parameters: headroom search lower bound, HR_{LB} , and upper bound HR_{UB} . Because 0% to 4% PV headroom is used in the

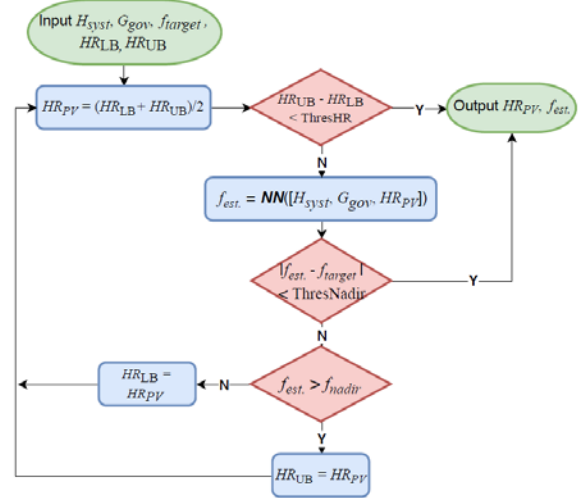


Fig. 8. Flow chart for binary searching algorithm.

training set, it is naturally to set $[HR_{LB}, HR_{UB}]$ as $[0\%, 4\%]$. If the algorithm is to be applied to a different system, the two bounds need to be re-evaluated.

After the input, the algorithm will start the search from the medium value of the upper and lower bounds, i.e. HR_{PV} . This medium value is used as the headroom and is send to the ANN model together with the input value of (H_{syst}, G_{gov}) to estimate the frequency nadir, f_{est} . If the f_{est} is equal to or close to the f_{target} , the search is terminated and the current HR_{PV} as well as the f_{est} are outputted. If f_{est} is larger than f_{target} , the upper bound is set to HR_{PV} , behind the rationale that the optimal headroom should be less than HR_{PV} . If f_{est} is smaller than f_{target} , the lower bound is set to HR_{PV} , behind the rationale that the optimal headroom should be less than HR_{PV} . After the bounds are updated, the search continues by updating the HR_{PV} to the medium.

Two parameters are introduced in this algorithm. The first is the ThresNadir, which is the criteria in determining that the f_{est} is equal to or close to the f_{target} . In this study, 0.001Hz is used. Another parameter is ThresHR, which terminates the search if the whole range of $[HR_{LB}, HR_{UB}]$ is searched but could not find a PV headroom so that f_{est} close enough to f_{target} . In this study, 0.01% of the PV headroom is used.

IV. DEMONSTRATION OF ONLINE APPLICATION

After the machine learning based strategy is trained offline, the next step is to demonstrate the strategy in the online application module. Because current system does not have such a high PV penetration level or the frequency control enabled, simulations that mimic the real system behavior are turned to.

The 1-day scenario shown in Fig. 4 is used. The profile comes with a 15-min interval and has a total of 96 intervals for the whole day. On this day, sunrise occurred at 5:00 and sunset at 19:30 which correspond to the input samples between the intervals 21 and 79. These 59 intervals are simulated.

Note that the ANN model has never seen this 1-day profile during its training or testing. For example, at 12:00, the system has an inertia of 281,377 MVA*s and an enabled governor

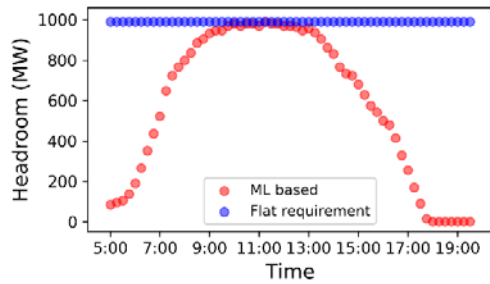


Fig. 9. Optimal headroom vs. conservative headroom.

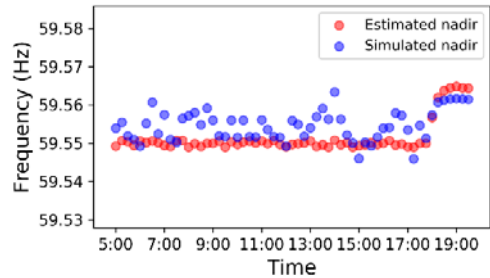


Fig. 10. Estimated vs. simulated frequency nadir.

capacity of 26,916 MVA, which is not in the training or testing set introduced in Section III A (also shown in Fig. 6).

In this demonstration, the f_{target} is chosen as 59.55 Hz. The under-frequency load-shedding in the WECC starts from 59.5 Hz. This target is set 0.05 Hz higher to give some margin for errors.

When the simulation advances to an interval: 1) the system inertia and enabled governor capacity of that interval along with the 59.55 Hz target are input to the algorithm to find the optimal PV headroom reserve; 2) the optimal PV headroom is deployed evenly to all PV power plants; and 3) the largest N-2 contingency is simulated in PSLF to find the actual frequency nadir to validate the effectiveness of the proposed strategy.

Fig. 9 shows the PV headroom determined through the proposed strategy (red dots) for all intervals. The headroom peaks around 1000 MW during the noon intervals when the system inertia is the lowest during the day (red line in Fig. 4). After 18:00, the optimal headroom found is 0 MW, which means that without the PV's support, the system frequency is greater than 59.55 Hz. The blue dots in Fig. 9 illustrate the strategy to use the highest PV headroom reserve, which is an over-conservative strategy if the online estimate algorithm is unavailable.

Fig. 10 depicts in red dots the estimated frequency nadir the proposed strategy found, and the simulated frequency nadir through PSLF is shown as blue dots. The average error is 0.004Hz with a standard deviation of 0.0029 Hz. Compared to the typical governor dead band of 0.036 Hz, the error is an order of magnitude smaller, which validates the performance of the proposed strategy.

On the other hand, compared with the conservative strategy shown in Fig. 9, the proposed strategy can realize a 41% PV headroom reduction/saving which equivalently allows PV to

produce 5,945 MWh more clean energy during this 1-day period.

V. CONCLUSIONS

This paper proposed a machine learning based PV headroom determination strategy for frequency control. The proposed strategy, which consists of an ANN regression model and a binary search algorithm, was trained on 1,987 offline simulation cases of the WECC system and achieved prediction results with errors an order of magnitude smaller than the typical governor control dead band. Furthermore, a demonstration of online application during a one-day period was performed to validate the effectiveness of the proposed strategy. The optimal PV headroom determined by the proposed strategy satisfied the desired frequency response of the operator and achieved more than 40% PV headroom savings compared with a conservative strategy at the same time. Future works include optimal distribution of the determined PV headroom and adaptive control parameters for frequency control.

ACKNOWLEDGMENT

This work was authored in part by the National Renewable Energy Laboratory, operated by Alliance for Sustainable Energy, LLC, for the U.S. Department of Energy (DOE) under Contract No. DE-AC36-08GO28308. Funding provided by the U.S. Department of Energy Solar Energy Technologies Office under Award Number 34321. The views expressed in the article do not necessarily represent the views of the DOE or the U.S. Government. The U.S. Government retains and the publisher, by accepting the article for publication, acknowledges that the U.S. Government retains a nonexclusive, paid-up, irrevocable, worldwide license to publish or reproduce the published form of this work, or allow others to do so, for U.S. Government purposes.

REFERENCES

- [1] G. L. Barbose, "U.S. Renewables Portfolio Standards: 2019 Annual Status Update," Jul. 2019.
- [2] G. Brinkman *et al.*, "Grid modeling for the SunShot vision study," National Renewable Energy Lab.(NREL), Golden, CO (United States), 2012.
- [3] Y. Liu, S. You, J. Tan, Y. Zhang, and Y. Liu, "Frequency Response Assessment and Enhancement of the U.S. Power Grids Toward Extra-High Photovoltaic Generation Penetrations—An Industry Perspective," *IEEE Transactions on Power Systems*, vol. 33, no. 3, pp. 3438–3449, May 2018.
- [4] M. Dreidy, H. Mokhlis, and S. Mekhilef, "Inertia response and frequency control techniques for renewable energy sources: A review," *Renewable and sustainable energy reviews*, vol. 69, pp. 144–155, 2017.
- [5] C. Loutan *et al.*, "Demonstration of essential reliability services by a 300-MW solar photovoltaic power plant," National Renewable Energy Lab.(NREL), Golden, CO (United States), 2017.
- [6] J. Tan, Y. Zhang, S. Veda, T. Elgindy, and Y. Liu, "Developing High PV Penetration Cases for Frequency Response Study of U.S. Western Interconnection," in *2017 Ninth Annual IEEE Green Technologies Conference (GreenTech)*, 2017, pp. 304–311.
- [7] "California ISO Open Access Same-time Information System (OASIS) site." [Online]. Available: <http://oasis.caiso.com>.
- [8] F. Pedregosa *et al.*, "Scikit-learn: Machine Learning in Python," *Journal of Machine Learning Research*, vol. 12, pp. 2825–2830, 2011.
- [9] Martín Abadi *et al.*, *TensorFlow: Large-Scale Machine Learning on Heterogeneous Systems*. 2015.
- [10] F. Chollet and others, "Keras: The Python Deep Learning library," 2015. [Online]. Available: <https://keras.io>.